



## ORIGINAL ARTICLE

# Analysis of hair components by nanoparticle-assisted laser desorption/ionization mass spectrometry imaging



Shu Taira <sup>a,\*</sup>, Hitomi Shikano <sup>a</sup>, Nobuyuki Takahashi <sup>b</sup>

<sup>a</sup> Faculty of Food and Agricultural Sciences, Fukushima University, 1 Kanayagawa, Fukushima City, Fukushima 960-1248, Japan

<sup>b</sup> YAC DASTech, Inc., 3-8-5 Bijogi, Toda City, Saitama 335-0031, Japan

Received 26 February 2022; accepted 14 August 2022

Available online 19 August 2022

## KEYWORDS

Chemical analysis;  
Hair treatment;  
Mass imaging;  
High-spatial resolution

**Abstract** Using a vertical hair-slice section, we compared the components of normal and damaged hair regions using two ionization methods, matrix-assisted laser desorption/ionization and nanoparticle-assisted laser desorption/ionization (Nano-PALDI) mass spectrometry. Nano-PALDI is useful for small-molecule and high spatial resolution (5  $\mu\text{m}$ ) analyses due to the lack of noise. Thus, clear images were obtained from thin hair samples. In Nano-PALDI mass spectrometry imaging, cystine and 18-methyleicosanoic acid as endogenous hair components localized in the cuticle and cortex and cuticle of normal hair, respectively. In contrast, both components were absent in damaged hair.

© 2022 The Author(s). Published by Elsevier B.V. on behalf of King Saud University. This is an open access article under the CC BY-NC-ND license (<http://creativecommons.org/licenses/by-nc-nd/4.0/>).

## 1. Introduction

Hair is an important organ that protects the head and helps regulate body temperature. Hair is composed of keratin proteins, lipids, and other molecules (HILTERHAUS-BONG and ZAHN, 1987). The part of a hair strand that extends outward from the scalp is called the shaft, and the part that extends inward is called the root. Hair contains an enormous amount of molecular information that is sensitive to chemical and physiologic influences. Because hair grows, it is possible to evaluate biological changes over time by analyzing hair samples from

the root to the shaft. Thus, hair samples can be used to obtain daily information non-invasively (Nakahara, 1999). Conventionally, we should divide hair as segment from tip to root and analyze the extracts of hair sample by liquid or gas chromatography technique (Villain et al., 2004, Alves et al., 2013). However, it is complicated to understand location of target molecules although this method could reveal components rate, quantitatively. Recently, mass spectrometry imaging (MSI) was adopted 2-dimensional hair analysis of time-course drug inoculation (Villain et al., 2004, Alves et al., 2013, Kamata et al., 2015, Kamata et al., 2020). In MSI experiment, we should prepare hair section by lengthwise or ring form. In addition, to recognize thin hair sample, high spatial resolution image is required.

In previous studies, we developed a nanoparticle-assisted laser desorption/ionization (Nano-PALDI) mass spectrometry MS method to ionize both small and large molecules without background signals in the low-mass region (Taira et al., 2012, 2014, Komori et al., 2015, Kuo et al., 2017, Pan et al., 2019) with high spatial resolution (Taira et al., 2008, Shiono and Taira 2020). Here, we attempted to visualize

\* Corresponding author.

E-mail address: [staira@agri.fukushima-u.ac.jp](mailto:staira@agri.fukushima-u.ac.jp) (S. Taira).

Peer review under responsibility of King Saud University.



Production and hosting by Elsevier

hair components using Nano-PALDI MSI methods to show high spatial resolution image. Two hair components are selected for visualization. Cystine is an important component of hair due to its involvement in the formation of disulfide bonds via two cysteine amino acid residues. Due to the high content of cystine, hair has the characteristics of being hard and elastic. 18-Methyleicosanoic acid (18-MEA) is a major component of the outer layer of the epicuticle of hair and functions in maintaining the hydrophobicity of the hair shaft surface and the shine and suppleness of hair. Cystine and 18-MEA are easily lost by chemical treatment of hair. Thus, as second experiment, we imaged bleached hair which was originally black hair to the borderline region between bleached and growing hair. In addition, to understand changes over time, hair sections were sliced lengthwise using a special slicing instrument. Using this slicer, we could prepare lengthwise hair sections without freezing or fixation with any reagent.

To demonstrate our methodology, in the present study, we compared the well-characterized matrix-assisted laser desorption/ionization (MALDI) MS method with Nano-PALDI in terms of ionization efficiency and spatial resolution for imaging hair components.

## 2. Experimental

### 2.1. Sample preparation

Bleach-treated and untreated black hair of females approximately 20 years old was used in the test. Collected hairs were set in a Bio-slicer (KATANA, YAC DASTech, Inc., Saitama, Japan) and sliced lengthwise. To identify the region between bleached and growing (black) hair, hair containing a borderline was sliced according to visual judgement. After preparation of hair sections, we confirmed the presence/absence of a borderline by optical microscopy. Cryofilm (type2C(9), SECTION-LAB, Hiroshima, Japan) was placed on ITO-coated glass slides (Bruker Daltonik GmbH, Germany) using double-sided tape (Norinopod Plus Co., Tokyo, Japan). The sliced hair was placed on the adhesive side with the cross section facing up. Optical images of the tissues were obtained using a microscope scanner (Nanozoomer, Hamamatsu Photonics, Shizuoka, Japan) before analysis by MALDI- or Nano-PALDI MS imaging (MSI).

### 2.2. Preparation of nanoparticles (NPs)

NPs were prepared by adding an aqueous solution of  $\text{FeCl}_2 \cdot 4\text{H}_2\text{O}$  (0.1 M; 20 mL) (FUJIFILM Wako Chemicals, Tokyo, Japan) to 20 mL of  $\gamma$ -aminopropyltriethoxysilane (Shin-Etsu Chemicals, Niigata, Japan). After stirring for 1 h at room temperature, the solution was centrifuged at 22,300 g (CF15RXII, Hitachi, Tokyo, Japan) at 4 °C for 1 h. The resulting precipitate was washed three times with ultrapure water. After washing, the NP precipitate was suspended in methanol.

### 2.3. MS and MSI by MALDI- and Nano-PALDI method

Two ionization methods, MALDI and Nano-PALDI, were used to detect and image target molecules. Target MS plates were coated with 10 mg  $\text{mL}^{-1}$  of  $\alpha$ -cyano-4-hydroxycinnamic acid (CHCA, Nacalai Tesque Inc., Kyoto, Japan) for MALDI or 10 mg  $\text{mL}^{-1}$  solution of the matrix NPs for Nano-PALDI. A 1.0- $\mu\text{L}$  aliquot of the standard, 10 pmol  $\mu\text{L}^{-1}$  of cystine (Tokyo Chemical Industry, Tokyo, Japan) or 18-MEA (FUJIFILM Wako Chemicals, Tokyo, Japan), in 80 % methanol

(residue-analysis grade, FUJIFILM Wako Chemicals) was added dropwise onto a coated plate. To confirm ionization of the standards, we used MALDI-TOF (rapifleX, Bruker Daltonik GmbH) for MS and MSI. To obtain tandem MS spectra, we used a collision-induced dissociation method.

For MALDI MSI, CHCA was sprayed on the hair tissue sections on ITO-coated glass slides using an automated pneumatic sprayer (TM-Sprayer, HTX Technologies, LLC). Ten spraying passes were made under the following conditions: flow rate, 120  $\mu\text{L}/\text{min}$ ; air flow, 10 psi; nozzle speed, 1,100 mm/min; temperature, 75 °C. For Nano-PALDI MSI, NPs were sprayed onto the hair tissue sections on the ITO-coated glass slides using an air brush (nozzle caliber, 0.2 mm).

After spraying the sections with an ionization-assisting reagent (CHCA or NPs), ionization in the laser spot areas was detected by scanning the sections. Mass spectra were acquired using a rapifleX (MALDI-TOF-MS) instrument and a 10-kHz pulse laser, and the laser spot areas (50 shots) were analyzed with a spot-to-spot center distance of 5  $\mu\text{m}$  in each direction on the section. Signals between  $m/z$  80–980 were collected. The tissue surface was irradiated with YAG laser shots in the positive ion detection mode. The laser power was optimized to minimize in-source decay of the targets. The obtained MS spectra were reconstructed to MS images with a mass bin width of  $m/z \pm 0.1$  from the exact mass using FlexImaging 5.1 software (Bruker Daltonik GmbH).

## 3. Results and discussion

### 3.1. Characterization of nanoparticle

The XRD pattern of the nanoparticles indicated that the very sharp peaks at  $2\theta = 35$  and  $63^\circ$  were confirmed to be the (1 3 0), (2 0 0) reflections and the (3 3 0), (0 6 0) reflections of macaulyite which was composed by iron oxide core. The FT-IR analysis (a) indicated the presence of O–H ( $3600$ – $3100$   $\text{cm}^{-1}$ ), C–H ( $2820$ – $2970$   $\text{cm}^{-1}$ ), C–N ( $1500$ – $1480$   $\text{cm}^{-1}$ ), and Si–O ( $1000$ – $800$   $\text{cm}^{-1}$ ) bonding as chemical bonds on the surface of the nanoparticles, even after several washing of the samples to remove physical adsorption of organic molecules. The diameter of the nanoparticle was measured to be  $3.6 \pm 0.06$  nm (mean  $\pm$  SEM;  $n = 300$ ) (Supporting information) (Taira et al., 2008).

### 3.2. Detection of hair components using Nano-PALDI-TOF-MS and MALDI-TOF-MS

Both Nano-PALDI and MALDI MS analysis of standard cystine and 18-MEA detected at  $m/z$  241.3 and 327.4, respectively, in the positive ion mode. The coefficients of determination ( $R^2$ s) of semilog plots of the signal intensity versus amount were relatively no difference between Nano-PALDI and MALDI indicating that both ionization methods have linearity. In Nano-PALDI, the limits of detection (LODs) of cystine and 18-MEA indicated 10 and 4.5 fmol, while those for MALDI were higher (Table 1). These results indicate that the sensitivity of Nano-PALDI is higher than that of MALDI.

Cystine and 18-MEA on hair sections were confirmed by tandem Nano-PALDI MS using the above-detected ions as precursor ions. As expected based on the chemical structure, a cystine fragment ion was observed at  $m/z$  152.0 from stan-

Compound	Nano-PALDI		MALDI	
	LOD (fmol)	R <sup>2</sup>	LOD (fmol)	R <sup>2</sup>
Cystine	10	0.981	45	0.991
18-MEA	4.5	0.978	25	0.982

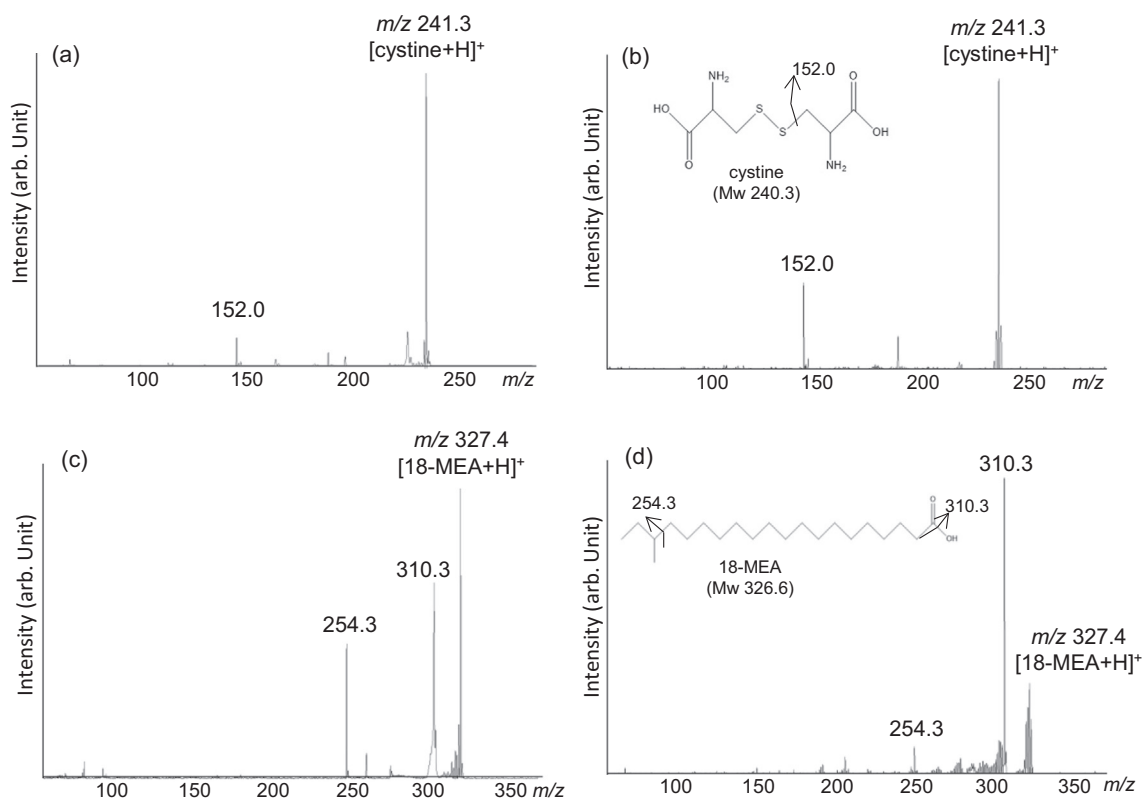
R<sup>2</sup> (coefficient of determination) was derived from semilog plots of signal intensity versus amount of each compounds. LOD: Limit of detection.

dard sample (Fig. 1a) and on section (Fig. 1b). 18-MEA fragment ions were observed at  $m/z$  310.3 and 254.3 from standard sample (Fig. 1c) and on section (Fig. 1d). We could confirmed exist of cystine and 18-MEA on section by Nano-PALDI MS. Because the  $m/z$  values of these fragmented ions on section were in good agreement with those of the respective standard samples (Fig. 1c and d). Detection of cystine may involve fragmentation from free cystine originally present in the hair or from proteins produced by laser irradiation of MS. Either way, cystine and 18-MEA are representative components to detect because it is an amino acid and lipid present in large amount in hair, reproducibly.

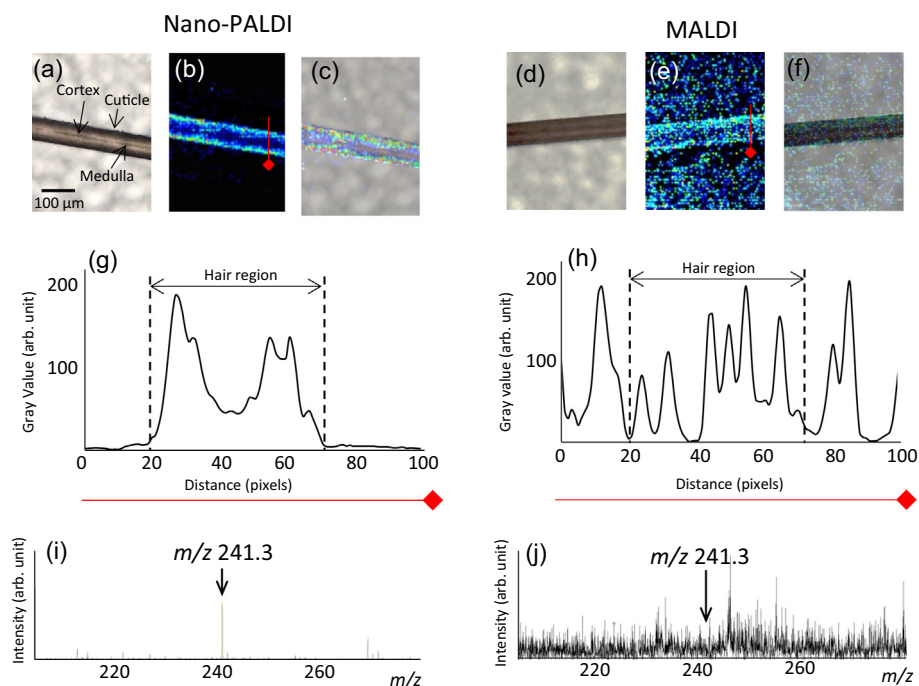
### 3.3. Comparison of Nano-PALDI and MALDI-MSI

Fig. 2 shows the results of Nano-PALDI and MALDI-MSI analyses of cystine detected on samples of non-treated black hair fiber. Hair sections were sliced longitudinally without embedding. Optical images provide information regarding

the hair region. The cuticle is localized as most outer layer. The cortex and medulla were confirmed as inner region and center of the hair fiber, respectively (Fig. 2a and d). To compare the spatial resolution, cystine was imaged by selecting  $m/z$  241.3 as the protonated cystine ion (Fig. 2b, e). For Nano-PALDI-MSI, we observed that cystine ( $m/z$  241.3) localized in the cuticle and cortex (Fig. 2b). MALDI-MSI also showed cystine localized in the cuticle and cortex, but the obtained images were blurry and exhibited background noise (Fig. 2e). We analyzed this difference by line profile analysis. Result in Nano-PALDI (Fig. 2g), line pattern indicated the lowest gray value at 0–20 and 80–100 pixels. On the other hand, two strong value areas observed at both end at hair region (20–70 pixels). The center of hair region as cortex showed broad value. In the case of MALDI (Fig. 2h), multiple peaks observed from all measured reason (0–100 pixels), especially strongest peak was detected at background region (0–20 and 70–100 pixels), indicating that matrix signal was higher than target signal and strongly involved high background sig-



**Fig. 1** Tandem mass spectra of standard (a) and on section (b) of cystine and standard (c) and on section (d) of 18-MEA.



**Fig. 2** MS imaging of a hair sample by Nano-PALDI (a-e) and MALDI (f-j). Optical image of hair fiber (a and d), MS image of protonated cystine ( $m/z$  241.3) by Nano-PALDI (b) and MALDI (e), merged images (c and f), line profile of MSI data by Nano-PALDI (g) and MALDI (h), and mass spectrum of hair section by Nano-PALDI (i) and MALDI (j).

nal. Notably, Nano-PALDI (Fig. 2b and g) MSI showed extreme lower background noise than that of MALDI (Fig. 2e and h). This difference in image quality was ascribed to the different characteristics of the ionization-assisting reagents. Our data suggest that only the target sample was ionized and the NPs themselves are not ionized in Nano-PALDI-MSI; therefore, no NP-derived signals are detected, resulting in a low-noise image. However, in the presence of organic matrix, both the matrix itself and the target sample are ionized (Shiono and Taira 2020). A common concern is that MALDI-based MSI is impractical for the imaging of low-molecular-weight targets due to the high background interference derived from organic matrices. In addition, MALDI, it is assumed that co-crystals formed by an organic matrix uniformly applied on the target surface are irradiated by the laser and ionized. Thus, for high-resolution images ( $<20 \mu\text{m}$ ), the construction of small size of the matrix crystals required by an automated pneumatic sprayer. On the other hand, in Nano-PALDI, we easily applied nanoparticle on section using manual air brush (nozzle caliber,  $0.2 \text{ mm}$ ) due to no need formation of co-crystals.

Hair section mass spectra are shown in Fig. 2i and j. The signal-to-noise ratio of Nano-PALDI (S/N 150) was 12.5 times higher than that of MALDI (S/N 12). Because MS spectrum in organic matrix showed several noises signal due to ionization of matrix itself. but NPs do not ionize itself. From line profile of images, Nano-PALDI showed lower background than that of MALDI. Nano-PALDI MSI is therefore suitable for imaging low molecular weight target molecules and small-sized samples.

### 3.4. Nano-PALDI-MSI of bleach-treated and untreated hair sections

We used a single hair fiber sample that could be divided into bleached and growing hair (untreated) regions at the center orange line. The term ‘untreated hair region’ refers to an area of new growth after bleaching. Fig. 3 shows Nano-PALDI-MSI data for cystine and 18-MEA in the bleach-treated and untreated regions. The optical images provide information on the bleached and untreated hair regions. The left side of the hair from the center is the bleached region, and the right side is the untreated region (Fig. 3a). Cystine was imaged by selecting  $m/z$  241.3 and found to be localized in the cuticle and cortex of the untreated hair region; toward the right side, there was more localization of cystine from the cuticle to the cortex (Fig. 3b and c). This could have been due to the fact that cystine, which is present in abundance within untreated hair, leaked out due to the damage-associated loss of hydrophobicity of the hair surface (Korte et al., 2014). From line profile analysis, in the bleached region (Fig. 3b-i-iii), cystine imaging intensity was only one-third that of the untreated region. The closer to the root, the intensity of cystine increased at cuticle and cortex region (Fig. 3b-iv-vi).

18-MEA was imaged by selecting  $m/z$  327.4 and found to be localized in the cuticle of the untreated hair region (Fig. 3d-x-xii and e). This result was in good agreement with a previous report that confirmed the localization of 18-MEA by atomic force microscopy (Tokunaga et al., 2019). In the bleach-treated region, 18-MEA was not imaged and not detected (Fig. 3d-vii-ix), although cystine was marginally imaged. We

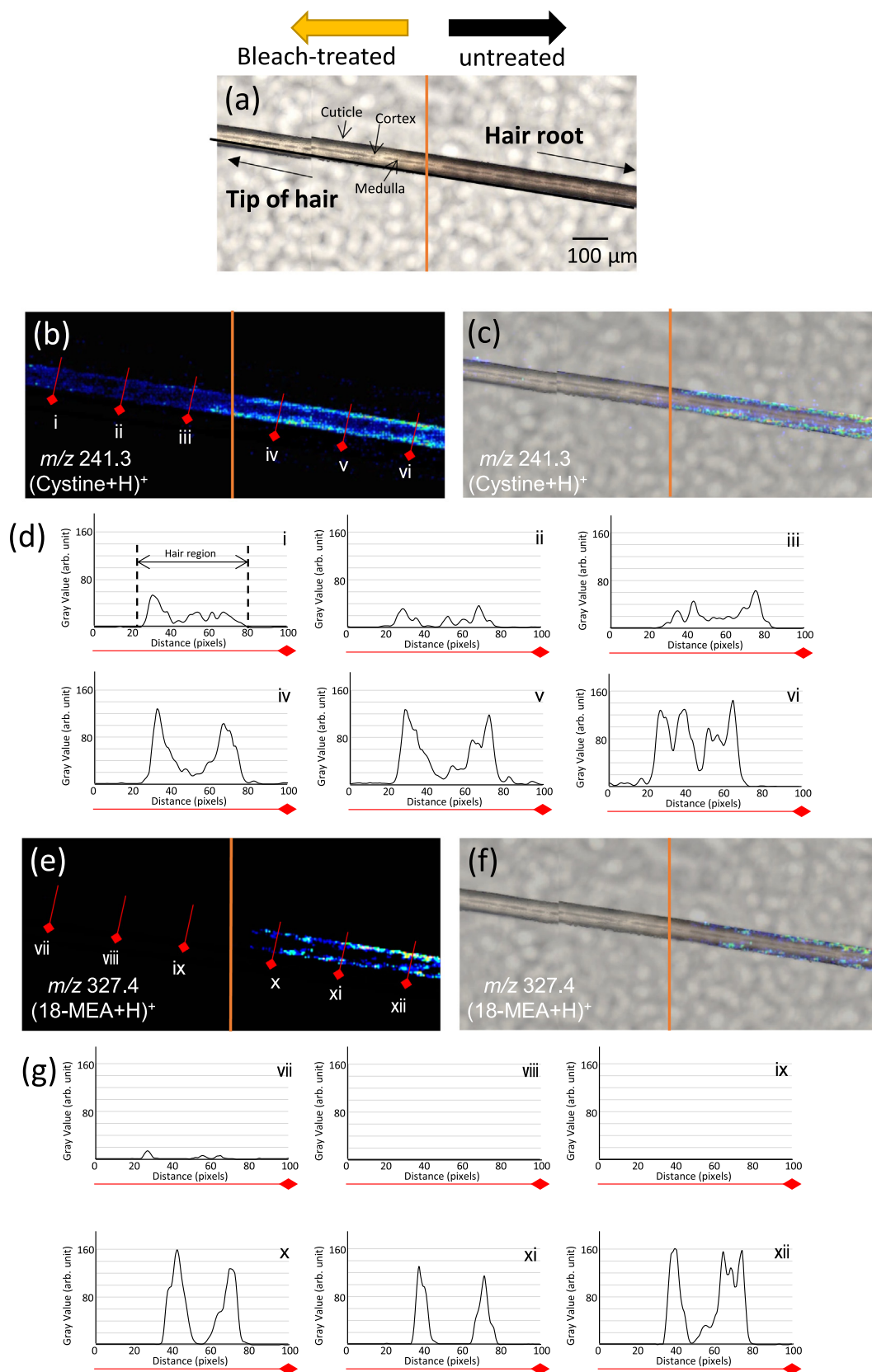


**Fig. 3** MS imaging evaluation of sample borderline by Nano-PALDI. Optical image of hair fiber (a), MS image of protonated cystine ( $m/z$  241.3) (b), merged image (c), line profile of cystine, MS image of protonated 18-MEA ( $m/z$  327.4) (e), merged image (f), line profile of 18-MEA (g).

hypothesis that the difference was attributed to the easier loss of 18-MEA than cystine from the hair surface, as occurs with chemical treatments such as coloring and bleaching due to that 18-MEA which is more hydrophobic than cystine affected chemical treatment. Nano-PALDI MSI gave us clear identifiable image of the boundary region.

#### 4. Conclusion

Until now, mass spectrometry imaging of hair has been performed using freeze-embedding or paraffin-embedding for sectioning, which results in the leakage of hydrophilic and hydrophobic components, respectively, from hair fibers, making it difficult to detect target substances (Miki et al., 2011, Waki et al., 2011). However, sectioning and ionization using the Bio-slicer and Nano-PALDI-MSI enable mass spectrometry with high spatial resolution with raw samples. Nano-PALDI MSI can also be used to acquire high-resolution images due to the absence of crystallization effects observed with MALDI. NPs are only physically adsorbed onto the sample surface, so even if the particles aggregate to form a secondary particle, the size is limited to approximately 100 nm in diameter (Taira et al., 2008). Therefore, MSI using the Nano-PALDI method can be easily performed with higher spatial resolution than that possible with conventional MALDI methods.

It is now possible to image and localize multiple components of hair fibers. We provided visual indications of the effects of chemical treatments such as bleaching on hair.

In future work, Nano-PALDI MSI will be applied not only to visualization in the cosmetics and healthcare industries but also to the identification of biomolecules and pharmaceutical components.

#### Declaration of Competing Interest

The authors declare that they have no known competing financial interests or personal relationships that could have appeared to influence the work reported in this paper.

#### Acknowledgement

This work was partly supported by the Japan Science and Technology (JST) Grants-in-A-STEP (VP30118067678 to S. T.) and the LOTTE foundation.

#### References

- Alves, M.N.R., Zanchetti, G., Piccinotti, A., et al, 2013. Determination of cocaine and metabolites in hair by column-switching LC-MS-MS analysis. *Anal. Bioanal. Chem.* 405, 6299–6306. <https://doi.org/10.1007/s00216-013-7046-3>.
- Hiltehaus-Bong, S., Zahn, H., 1987. Contributions to the chemistry of human hair. 1. Analyses of cystine, cysteine and cystine oxides in untreated human hair. *Int. J. Cosmet. Sci.* 9, 101–110. <https://doi.org/10.1111/j.1467-2494.1987.tb00467.x>.
- Kamata, T., Shima, N., Sasaki, K., et al, 2015. Time-Course Mass Spectrometry Imaging for Depicting Drug Incorporation into Hair. *Anal. Chem.* 87, 5476–5481. <https://doi.org/10.1021/acs.analchem.5b00971>.
- Kamata, T., Shima, N., Miki, A., et al, 2020. High Spatial-Resolution Matrix-Assisted Laser Desorption/Ionization-Ion Trap-Time-of-Flight Tandem Mass Spectrometry Imaging for Depicting Longitudinal and Transverse Distribution of Drugs Incorporated into Hair. *Anal. Chem.* 92, 5821–5829. <https://doi.org/10.1021/acs.analchem.9b05401>.
- Komori, H., Hashizaki, R., Osaka, I., et al, 2015. Nanoparticle-assisted laser desorption/ionization using sinapic acid-modified iron oxide nanoparticles for mass spectrometry analysis. *Analyst.* 140, 8134–8137. <https://doi.org/10.1039/C5AN02081F>.
- Korte, M., Akari, S., Kühn, H., et al, 2014. Distribution and Localization of Hydrophobic and Ionic Chemical Groups at the Surface of Bleached Human Hair Fibers. *Langmuir* 30, 12124–12129. <https://doi.org/10.1021/la500461y>.
- Kuo, T.-R., Chen, Y.-C., Wang, C.-I., et al, 2017. Highly oriented Langmuir-Blodgett film of silver cuboctahedra as an effective matrix-free sample plate for surface-assisted laser desorption/ionization mass spectrometry. *Nanoscale.* 9, 11119–11125. <https://doi.org/10.1039/C7NR04098A>.
- Miki, A., Katagi, M., Kamata, T., et al, 2011. MALDI-TOF and MALDI-FTICR imaging mass spectrometry of methamphetamine incorporated into hair. *J. Mass Spectrometry.* 46, 411–416. <https://doi.org/https://doi.org/10.1002/jms.1908>.
- Nakahara, Y., 1999. Hair analysis for abused and therapeutic drugs. *J. Chromatogr. B Biomed. Sci. Appl.* 733, 161–180. [https://doi.org/10.1016/S0378-4347\(99\)00059-6](https://doi.org/10.1016/S0378-4347(99)00059-6).
- Pan, X.-Y., Chen, C.-H., Chang, Y.-H., et al, 2019. Osteoporosis risk assessment using multilayered gold-nanoparticle thin film via SALDI-MS measurement. *Anal. Bioanal. Chem.* 411, 2793–2802. <https://doi.org/10.1007/s00216-019-01759-5>.
- Shiono, K., Taira, S., 2020. Imaging of Multiple Plant Hormones in Roots of Rice (*Oryza sativa*) Using Nanoparticle-Assisted Laser Desorption/Ionization Mass Spectrometry. *J. Agric. Food. Chem.* 68, 6770–6775. <https://doi.org/10.1021/acs.jafc.0c00749>.
- Taira, S., Sugiura, Y., Moritake, S., et al, 2008. Nanoparticle-assisted laser desorption/ionization based mass imaging with cellular resolution. *Anal. Chem.* 80, 4761–4766. <https://doi.org/10.1021/ac800081z>.
- Taira, S., Osaka, I., Shimma, S., et al, 2012. Oligonucleotide analysis by nanoparticle-assisted laser desorption/ionization mass spectrometry. *Analyst.* 137, 2006–2010.
- Taira, S., Taguchi, H., Fukuda, R., et al, 2014. Silver Oxide Based Nanoparticle Assisted Laser Desorption/Ionization Mass Spectrometry for the Detection of Low Molecular Weight Compounds. *Mass Spectrometry.* 3, S0025. <https://doi.org/10.5702/massspectrometry.S0025>.
- Tokunaga, S., Tanamachi, H., Ishikawa, K., 2019. Degradation of Hair Surface: Importance of 18-MEA and Epicuticle. *Cosmetics* 6, 31.
- Villain, M., Cirimele, V., Kintz, P., 2004. Hair analysis in toxicology. *Clin. Chem. Laborat. Med. (CCLM)* 42, 1265–1272. <https://doi.org/10.1515/CCLM.2004.247>.
- Waki, M.L., Onoue, K., Takahashi, T., et al, 2011. Investigation by Imaging Mass Spectrometry of Biomarker Candidates for Aging in the Hair Cortex. *PLoS ONE* 6, e26721.